Supporting Information

Role of Intermolecular Charge Transfer towards Fluorometric Detection of Fluoride Ion with Anthrapyrazolone Derivatives

Gomathi Sivakumar[a], Anashwara Babu[a], Anubhab Das[a], Mageshwari Anandhan[a], Venkatramaiah Nutalapati[a]* and Samarendra Maji[a]*

[a]Department of Chemistry, Faculty of Engineering and Technology, SRM Institute of Science and Technology (SRMIST), Kattankulathur, Tamil Nadu- 603203, India.

*Corresponding author E-mail: *nvenkat83@gmail.com/venkatrv1@srmist.edu.in*, *samarenr@srmist.edu.in*

1. Characterization

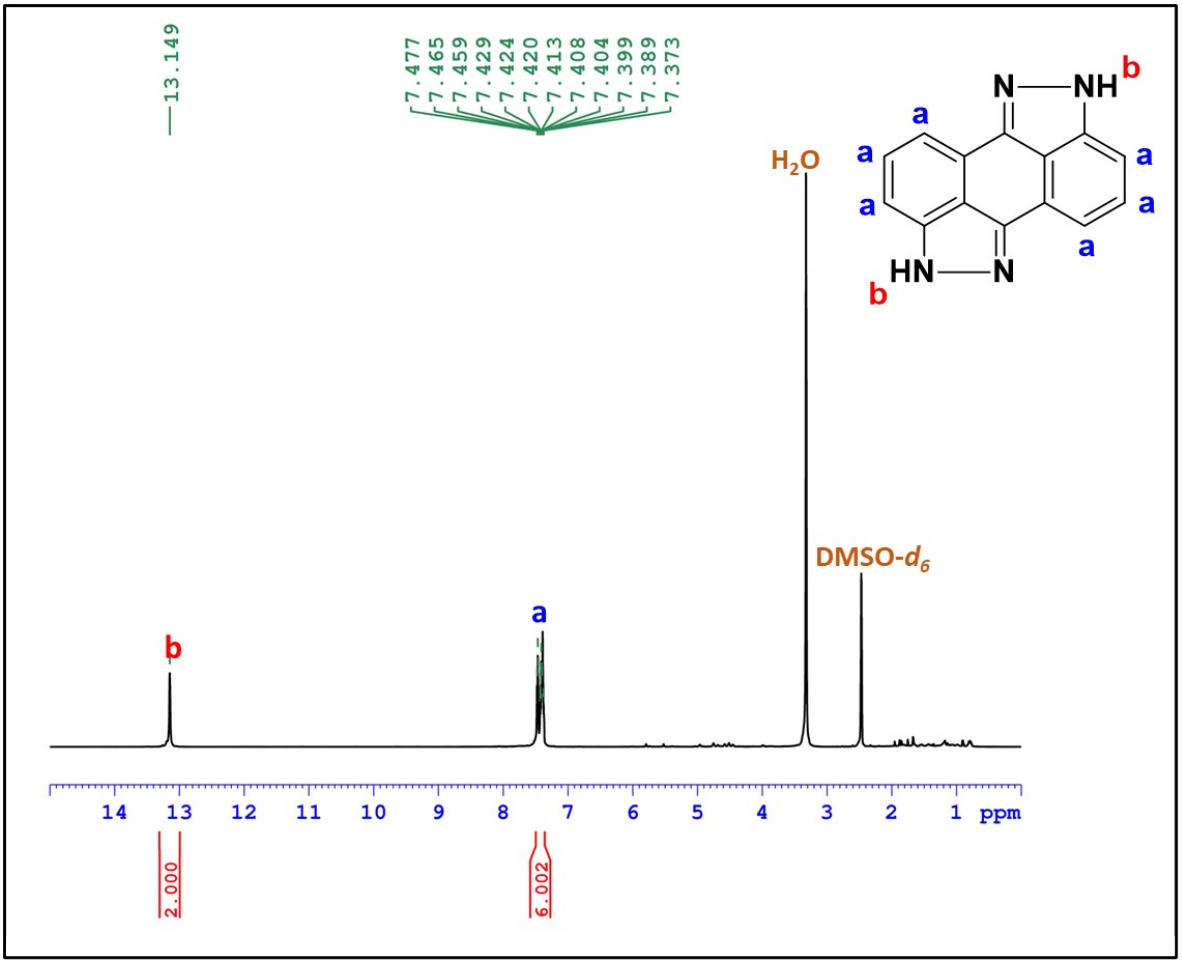

Fig. S1. ^{1}H NMR spectrum of DHBBI, measured in DMSO-d_6

^{1}H NMR (500 MHz, DMSO-d_6) δ ppm: 13.149 (s, 2H), 7.47 – 7.37 (m, 6H).

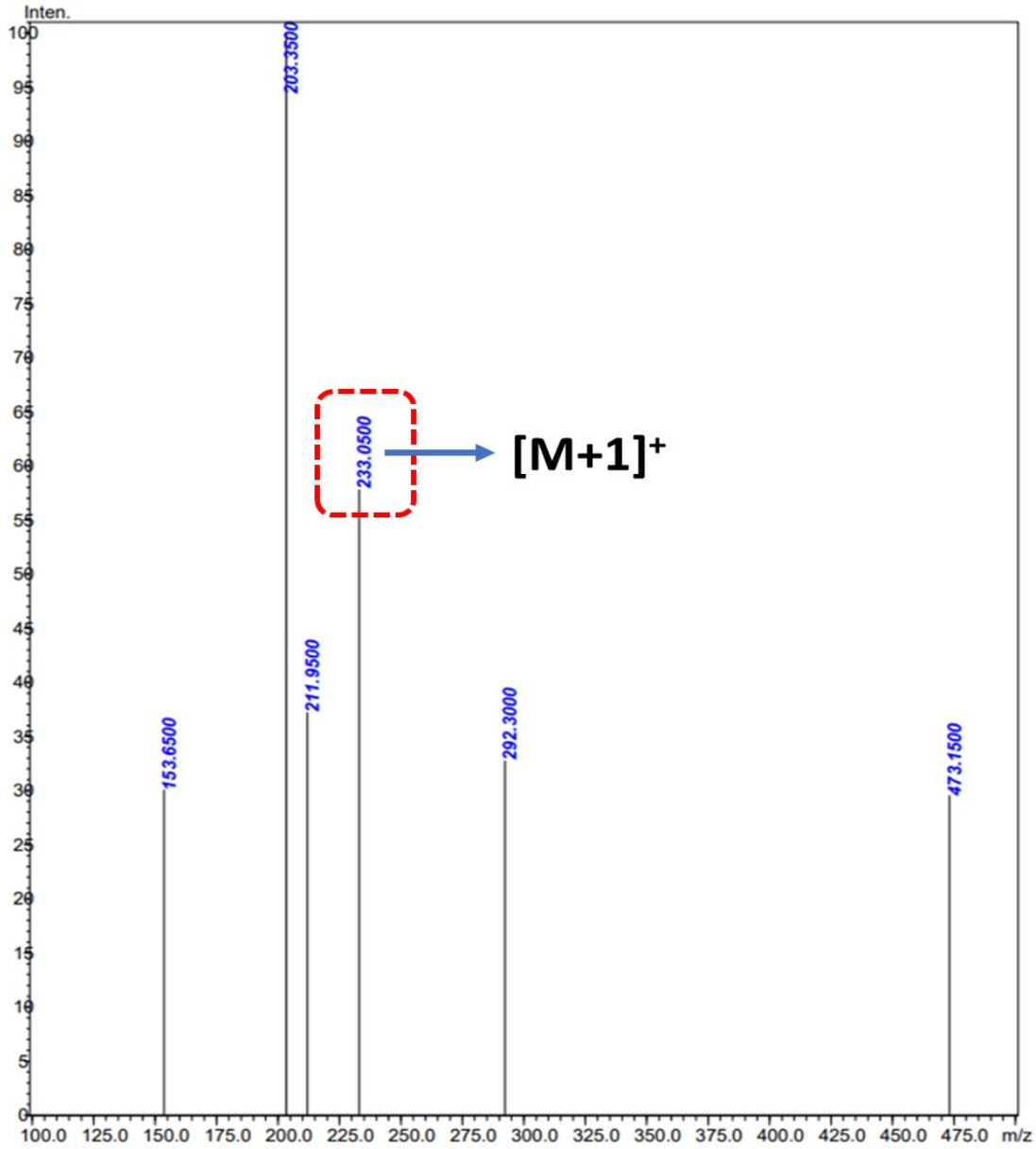

Fig. S2. ESI Mass spectrum of DHBBI.

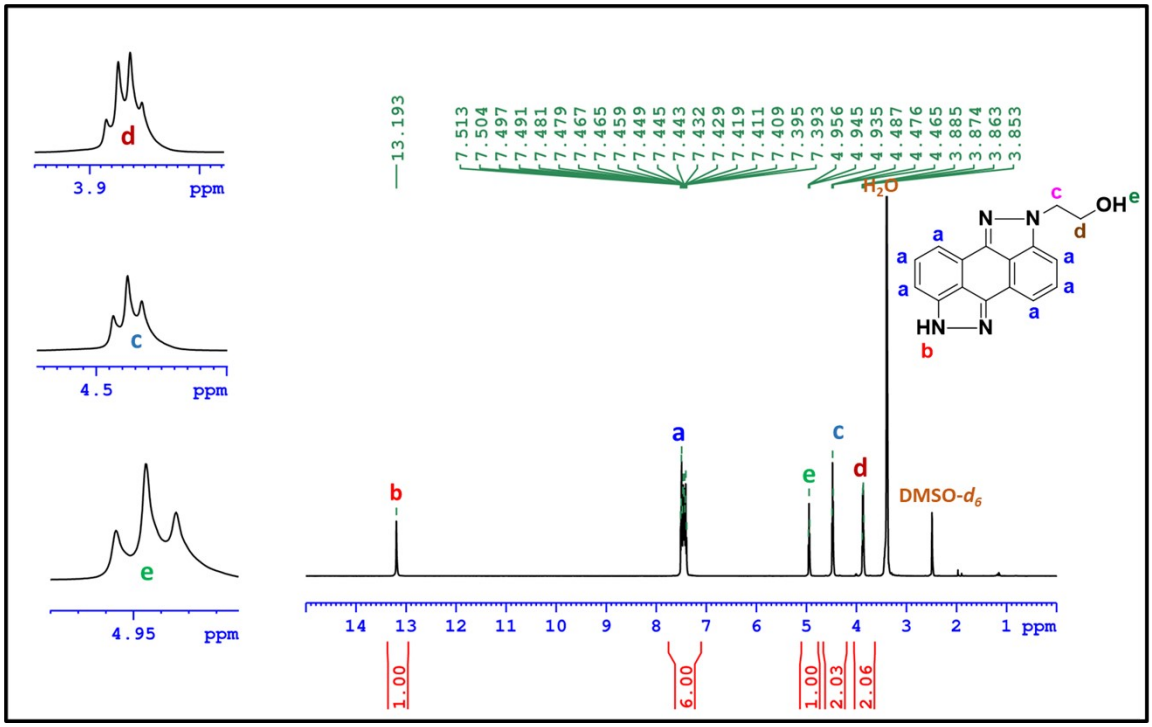

Fig. S3. ^{1}H-NMR spectrum of DHBBI-OH, measured in DMSO-d_6.

^{1}H-NMR (500 MHz, DMSO-d_6) δ ppm: 13.19 (s, 1H), 7.51 – 7.40 (m, 6H), 4.97 (t, J = 5.1 Hz, 1H), 4.50 (t, J = 5.4 Hz, 2H), 3.89 (q, J = 5.6 Hz, 2H).

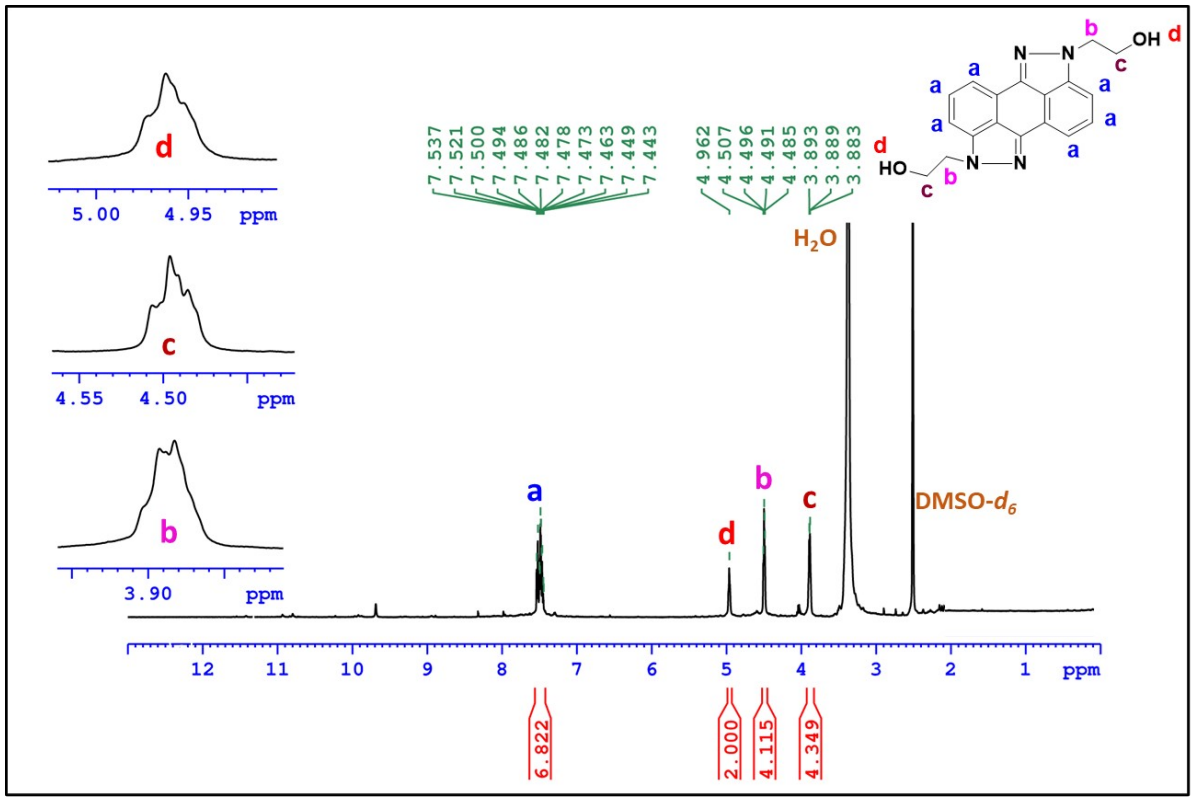

Fig. S4. ^{1}H NMR spectrum of DHBBI-2-OH, measured in DMSO-d_6.

^{1}H NMR (500 MHz, DMSO-d_6) δ ppm: 7.53 – 7.44 (m, 6H), 4.9 (t, J = 4.75 Hz, 2H), 4.490 (t, J = 5.45 Hz, 4H), 3.89 (q, J = 5.5 Hz, 4H)

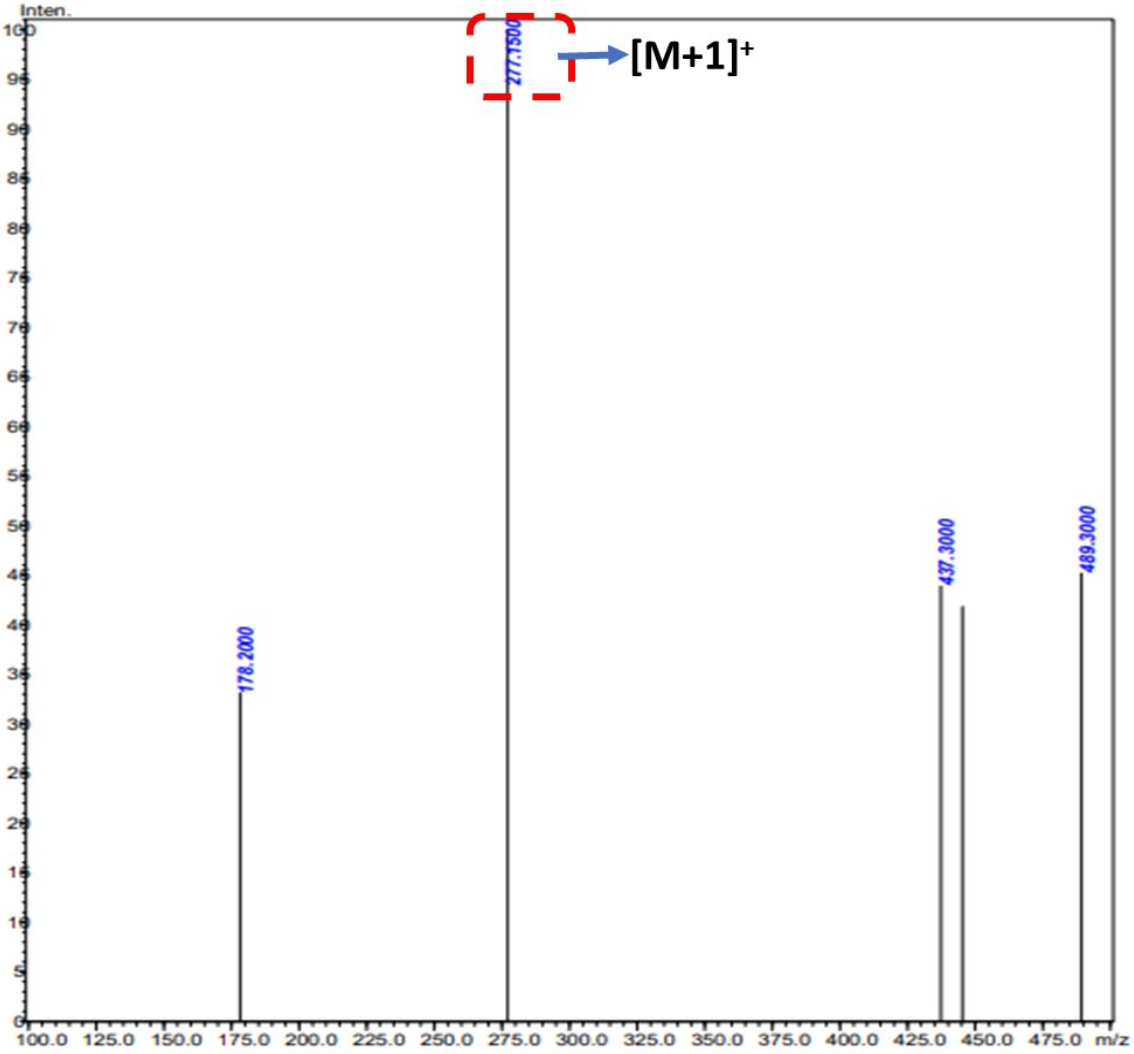

Fig. S5. ESI Mass spectrum of DHBBI-OH.

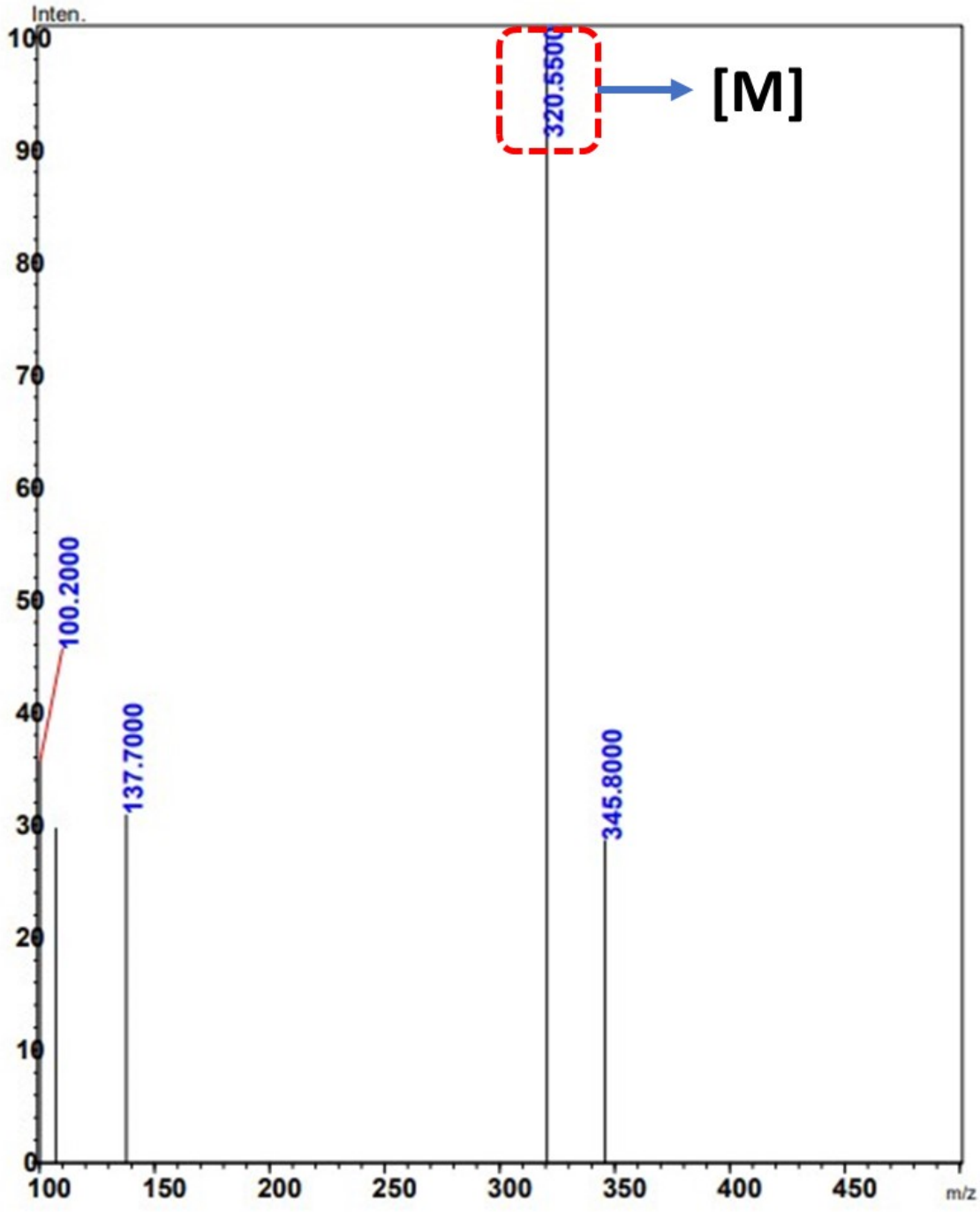

Fig. S6. ESI Mass spectrum of DHBBI-2-OH.

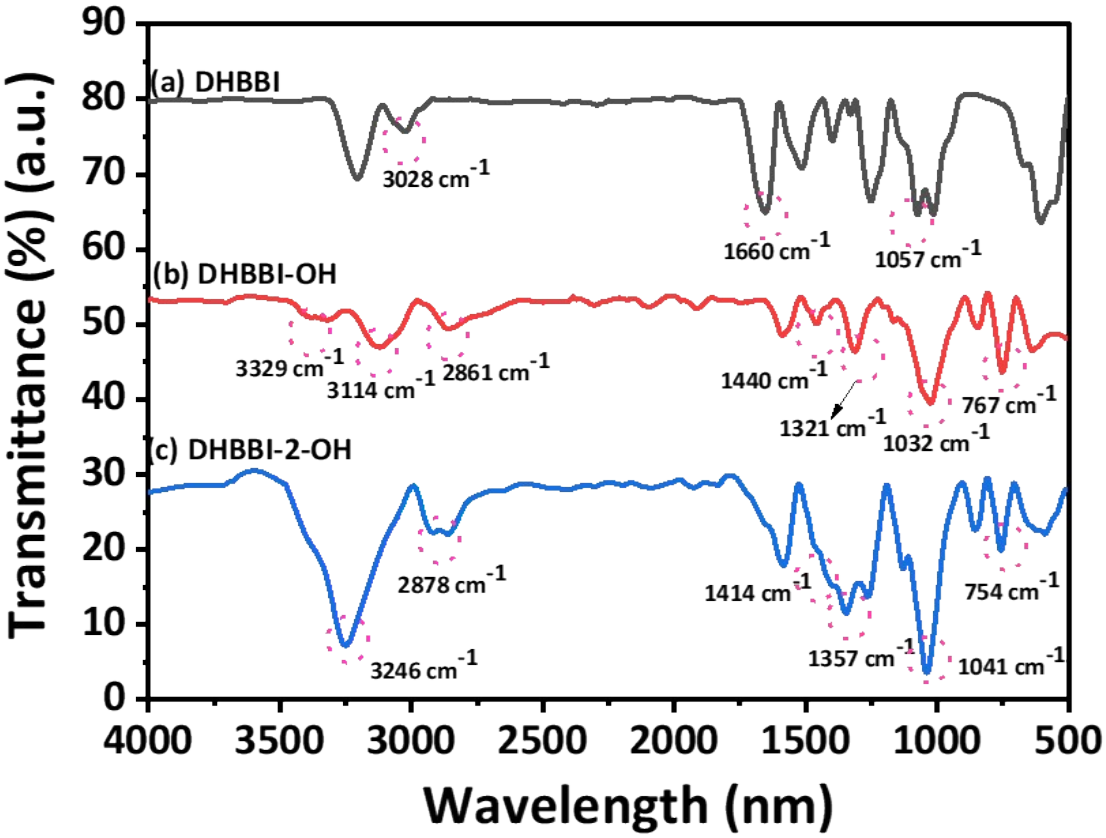

Fig. S7. FTIR spectra of DHBBI, DHBBI-OH and DHBBI-2-OH.

Table S1. Selected Bond parameters of compounds DHBBI, DHBBI-OH, and DHBBI-2-OH from DFT studies.

Atom No.	DHBBI	DHBBI-OH	DHBBI-2-OH
	Bond lengths (Å)		
C1-H19, C11-H24, C5-H21, C13-H22	1.082	≈1.085	1.083
C6-H20, C12-H23	1.084	1.084	1.084
C7-C3, C9-C8	1.432	1.432	1.430
C8-C4, C10-C7	1.459	1.458	1.458
C10=C9, C4-C3, C2-C1, C13=C14	1.406	1.406	1.406
C3=C2, C9-C14	1.403	1.403	1.403
C1=C6, C13-C12	1.395	1.395	1.395
C6-C5, C12=C11	1.415	1.415	1.415
C5=C4, C11-C10	1.393	1.393	1.393
C7=N17, C8=N16	1.337	1.337	1.338
C2-N18, C14-N15	1.381	1.381±2	1.382
N16-N15, N17- N18	1.418	1.418, 1.421	1.420
N18-H26, N15-H25	1.010	-	-
N18-C26	-	1.461	1.460
C26-C29	-	1.547	1.533
C26-H27, C26-H28, C29-H30, C29-H31	-	1.099	-
C25-H26, C25-H27, C33-H34, C33-H35	-	-	1.092
C28-H29, C28-H30, C36-H37, C36-H38	-	-	1.097
C29-O33	-	1.456	-
O33-H32	-	0.995	-
C28-O31, C36-O39	-	-	1.458

O31-H32, O39-H40			1.093
	Bond angles		
H25-N15-N16	117.98	117.98	-
H26-N18-N17	117.98	-	-
N16-C8-C4	130.93	130.92	131.17
N17-C7-C10	130.93	131.11	131.17
H26-N18-C2	179.94	-	-
H25-N15-C14	179.94	179.94	-
C26-N18-N17	-	117.96	-
C26-C29-O32	-	110.30	-
H33-O32-O29	-	107.56	-
C26-N18-C2	-	130.22	-
C25-N15-N16, C33-N18-N17	-	-	118.22
C25-C28-O31, C33-C36-O39	-	-	147.76
H40-O39-C36, H32-O31-C28	-	-	108.13
	Dihedral angle		
H26-N18-N17-C7	179.98	-	-
N17-C7-C10-C9, N16-C8-C4-C3	179.99	179.92	179.92
C7-N17-N18-C2	0.00487	0.462	0.3461
C8-N16-N5-C14	0.00435	0.00390	0.3462
C4-C3-C7-C10	0.00026	0.00846	0.06836
C1-C6-C5-C4	0.00148	0.0423	0.01242
H22-C13-C12-H23	0.03292	0.00458	0.0133
H19 -C1-C6-H20	0.00734	0.1154	0.0133
N17-N18-C26-C29	-	65.79	-
N18-C26-C29-O32	-	175.21	-
H27-C26-C29-H31	-	60.55	-

H31-C29-O32-H33	-	49.78	-
C26-N18-N17-C7	-	176.99	-
N16-N15-C25-C28, N17-N18-C33-C36	-	-	53.39
O31-C28-C25-N15, N18-C33-C36-O39	-	-	179.98

Table S2. Absorption spectra data obtained by TD-DFT methods for DHBBI, DHBBI-OH and DHBBI-2-OH compounds at B3LYP/6-31g* (d,p) optimized geometries.

Compounds	Electronic transition	E (eV)	λ (nm) (theo.)	Oscillator strength (f)	Composition	Major contribution
DHBBI	$S_0 \rightarrow S_1$	3.4391	360.51	0.3703	HOMO → LUMO	97.3
DHBBI-OH	$S_0 \rightarrow S_1$	3.3510	369.99	0.3978	HOMO → LUMO	97.39
	$S_0 \rightarrow S_2$	4.0108	309.13	0.0027	HOMO-3 → LUMO HOMO-1 → LUMO HOMO→ LUMO+1	5.14 85.54 4.93
	$S_0 \rightarrow S_3$	4.3748	283.40	0.0002	HOMO-3 → LUMO HOMO-1 → LUMO HOMO → LUMO+1	11.56 3.73 80.30
DHBBI-2-OH	$S_0 \rightarrow S_1$	3.2887	377.01	0.4325	HOMO → LUMO	97.93

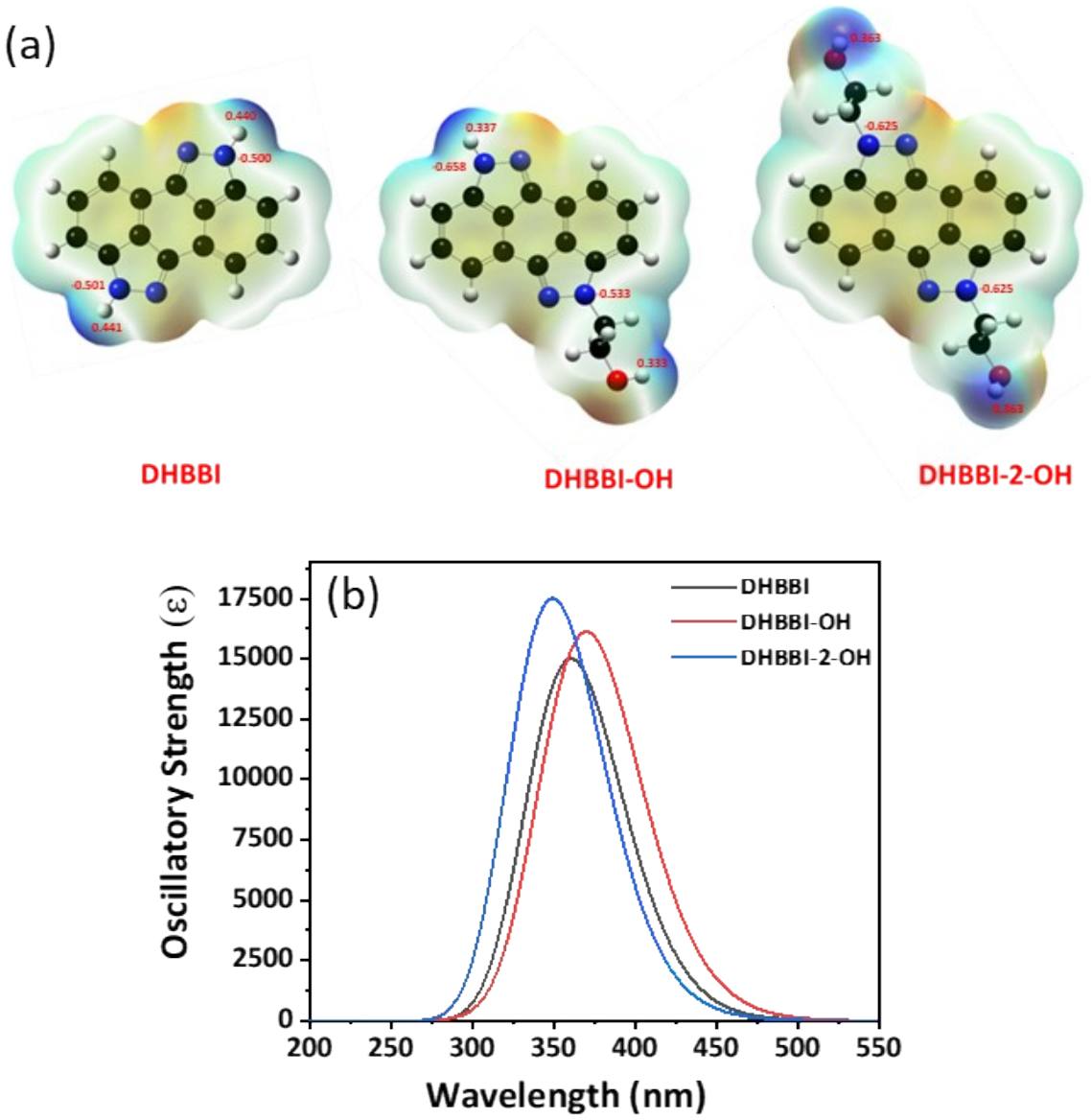

Fig. S8. (a) Calculated electrostatic potential surfaces on the molecular surfaces and (b) Calculated UV-Vis spectra of DHBBI, DHBBI-OH, and DHBBI-2-OH at B3LYP/6-31g*(d,p).

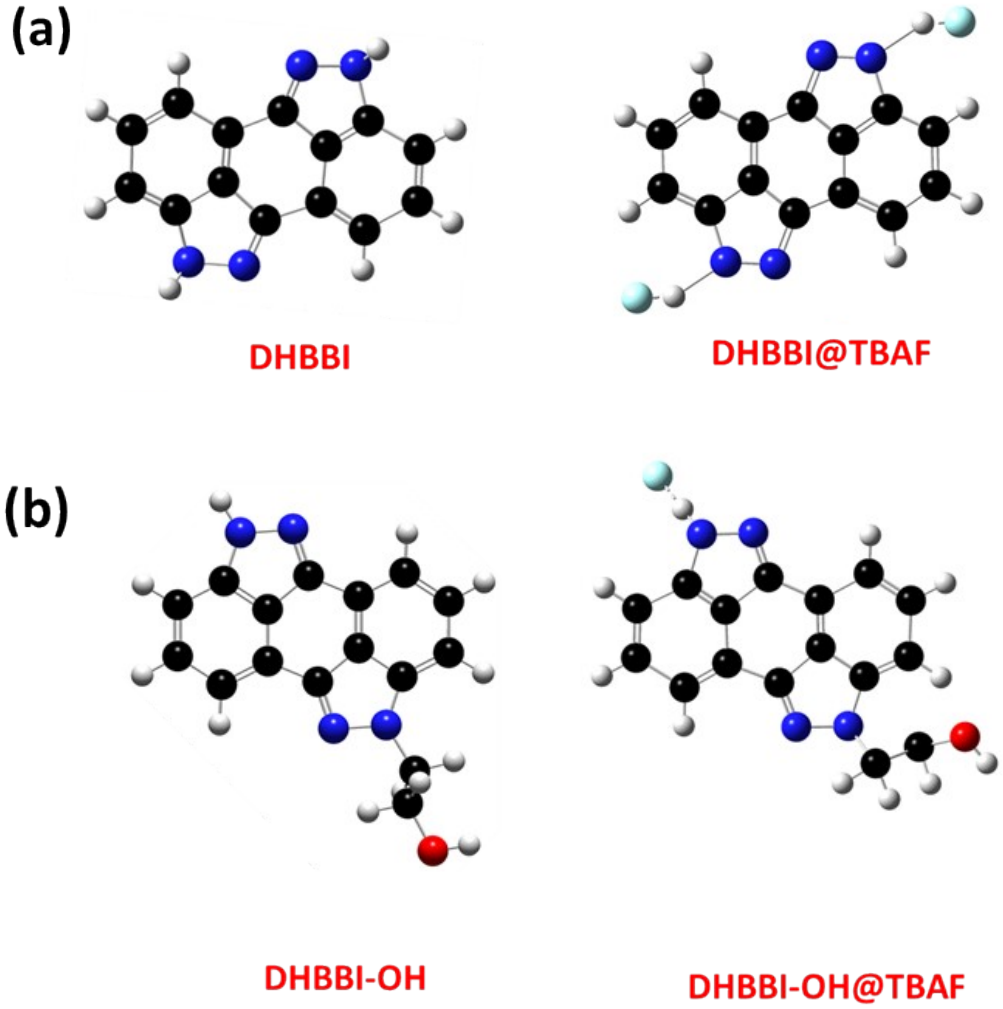

Fig. S9. Optimized geometry of complexation of TBAF with (a) DHBBI and (b) DHBBI-OH molecule obtained using DFT/B3LYP/6-31g* theoretical mode.

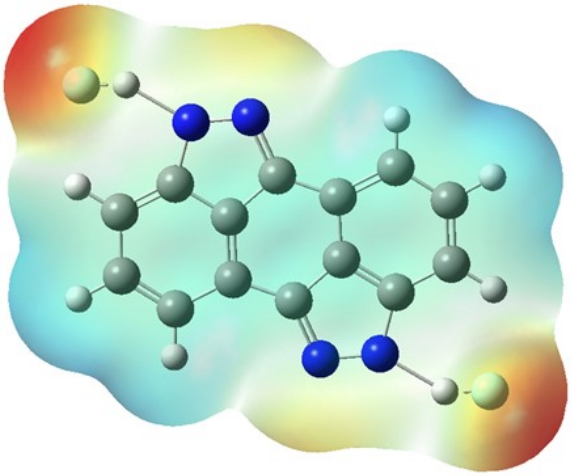

DHBBI@TBAF

Fig. S10. Calculated electrostatic potential surfaces on the molecular surfaces of complexation of TBAF, TBACN and TBAOH with DHBBI.

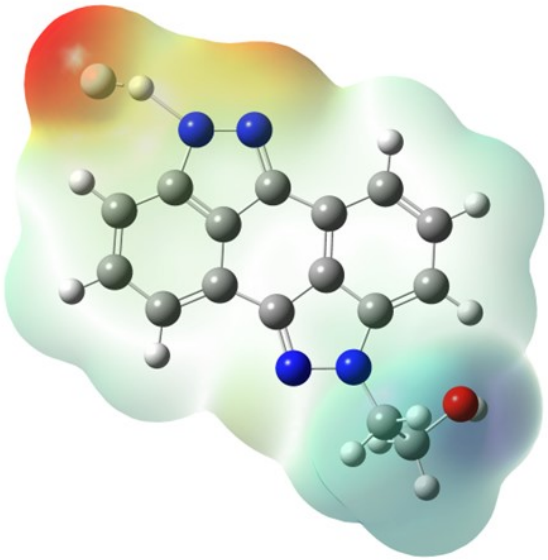

Fig. S11. Calculated electrostatic potential surfaces on the molecular surfaces of complexation of TBAF, TBACN and TBAOH with DHBBI-OH.

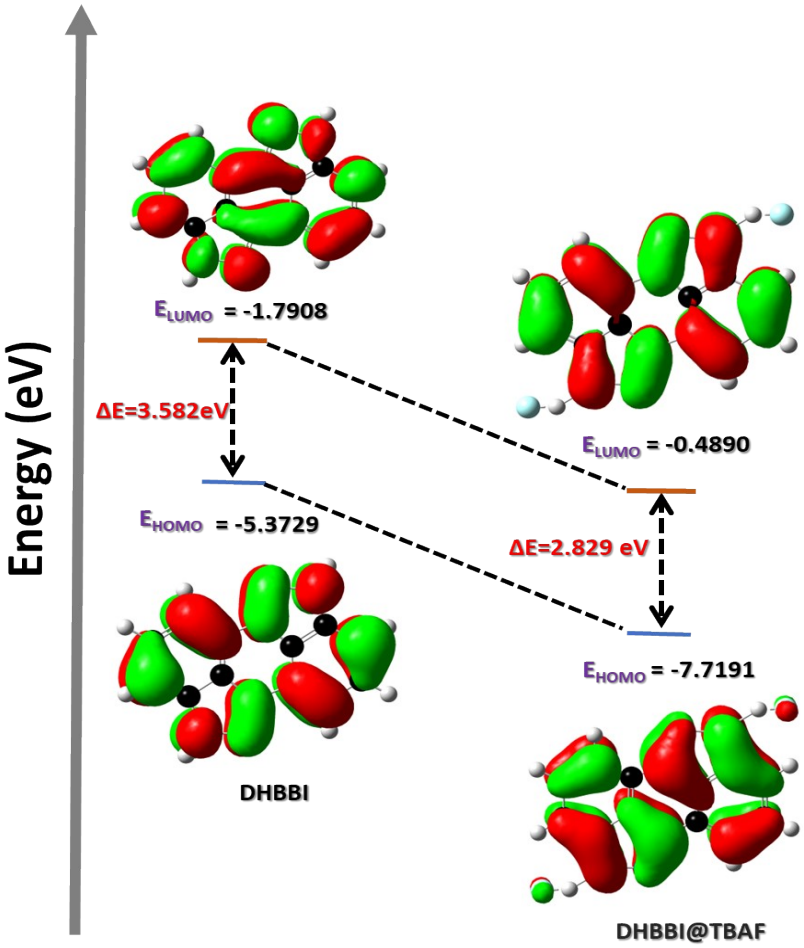

Fig. S12. Energy profile diagram showing variation in the HOMO and LUMO gap on complexation of TBAF with DHBBI.

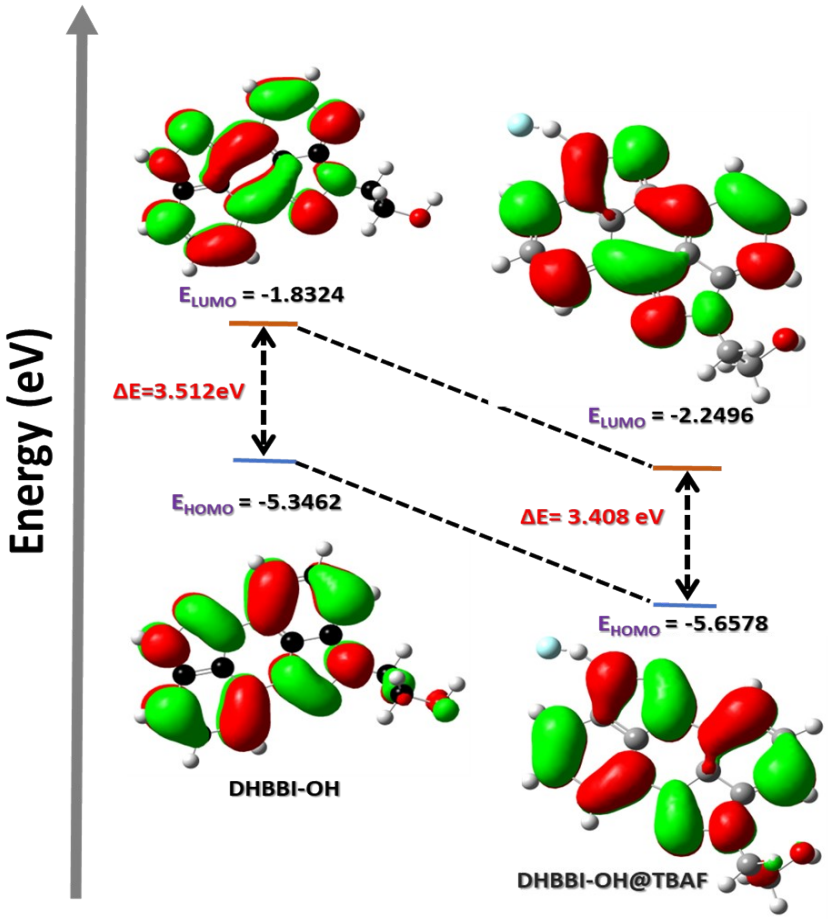

Fig. S13. Energy profile diagram showing variation in the HOMO-LUMO gap on complexation of TBAF with DHBBI-OH.

Table S3. Absorption spectra data obtained by TD-DFT methods for TBAF, TBACN and TBAOH complex with DHBBI compound at B3LYP/6-31g* (d,p) optimized geometries.

Compounds	Electronic transition	E (eV)	λ (nm) (theo.)	Oscillator strength (f)	Composition	Major contribution
DHBBI	$S_0 \rightarrow S_1$	3.4391	360.51	0.3703	HOMO → LUMO	97.3
DHBBI@ TBAF	$S_0 \rightarrow S_2$	2.2500	551.03	0.0014	HOMO-2→ LUMO	98.40
	$S_0 \rightarrow S_3$	2.4088	514.72	0.0063	HOMO-5 → LUMO HOMO-3 → LUMO	7.78 90.66

Table S4. Absorption spectra data obtained by TD-DFT methods for TBAF, TBACN, and TBAOH complex with DHBBI-OH compound at B3LYP/6-31g* (d,p) optimized geometries.

Compounds	Electronic transition	E (eV)	λ (nm) (theo.)	Oscillator strength (f)	Composition	Major contribution
DHBBI-OH	$S_0 \rightarrow S_1$	3.3510	369.99	0.3978	HOMO → LUMO	97.39
	$S_0 \rightarrow S_2$	4.0108	309.13	0.0027	HOMO-3 → LUMO HOMO-1 → LUMO HOMO → LUMO+1	5.14 85.54 4.93
	$S_0 \rightarrow S_3$	4.3748	283.40	0.0002	HOMO-3 → LUMO HOMO-1 → LUMO HOMO → LUMO+1	11.56 3.73 80.30
DHBBI-OH @TBAF	$S_0 \rightarrow S_1$	1.7201	720.81	0.0391	HOMO-8 → LUMO HOMO-6 → LUMO HOMO-3→LUMO HOMO-1 → LUMO HOMO → LUMO LUMO → HOMO	8.60 2.67 17.51 17.42 49.93 2.40
	$S_0 \rightarrow S_2$	1.9957	621.25	0.0329	HOMO-9 → LUMO HOMO-3 → LUMO HOMO-2→LUMO HOMO-1 → LUMO HOMO → LUMO	2.10 5.78 19.28 33.24 36.04
	$S_0 \rightarrow S_3$	2.2500	551.05	0.0139	HOMO-9 → LUMO HOMO-8 → LUMO	20.04 2.21

					HOMO-3→LUMO	10.89
					HOMO-2 → LUMO	50.49
					HOMO-1 → LUMO	2.56
					HOMO → LUMO	9.39

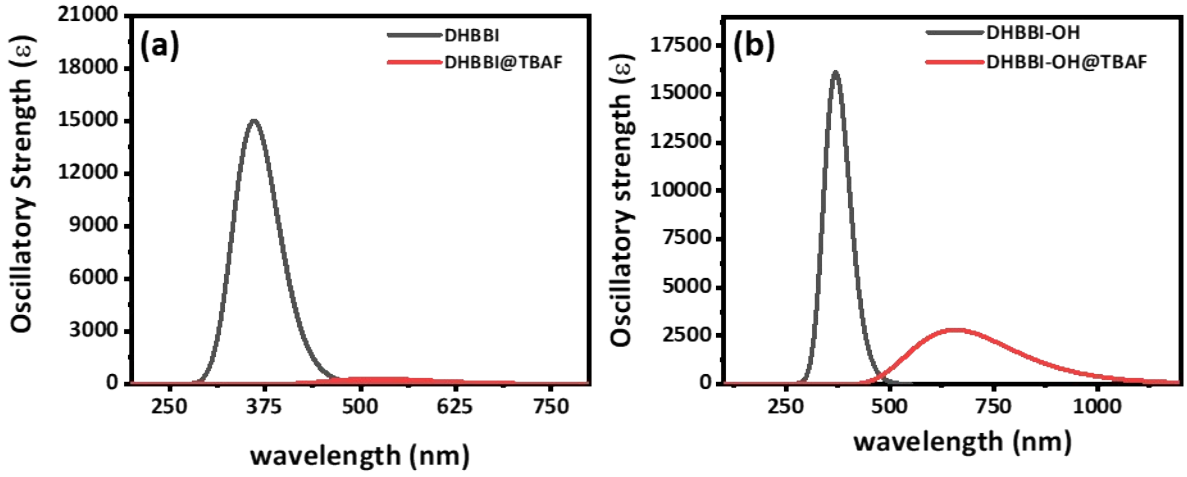

Fig. S14. Calculated UV-Vis spectra of TBAF complexes of (a) DHBBI and (b) DHBBI-OH at B3LYP/6-31g*(d,p).

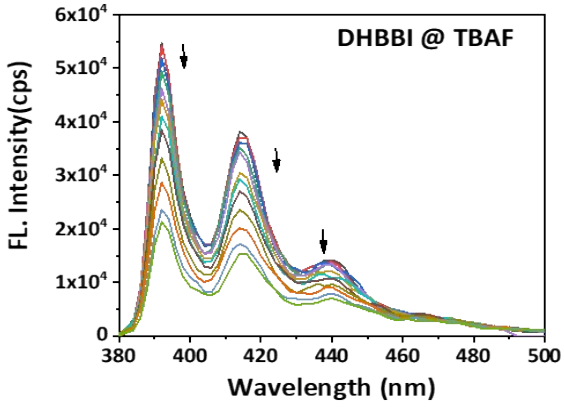
DHBBI @ TBAF
FL. Intensity(cps)
Wavelength (nm)

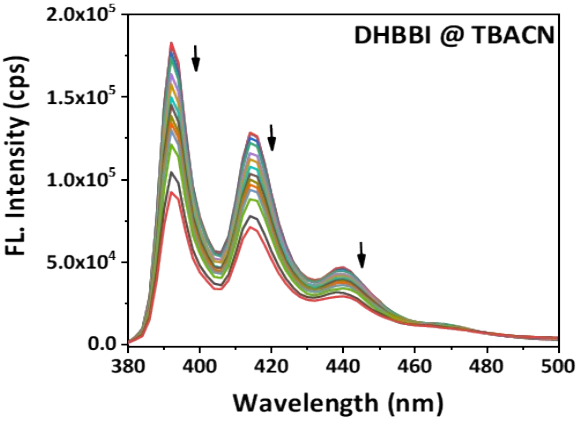
DHBBI @ TBACN
FL. Intensity (cps)
Wavelength (nm)

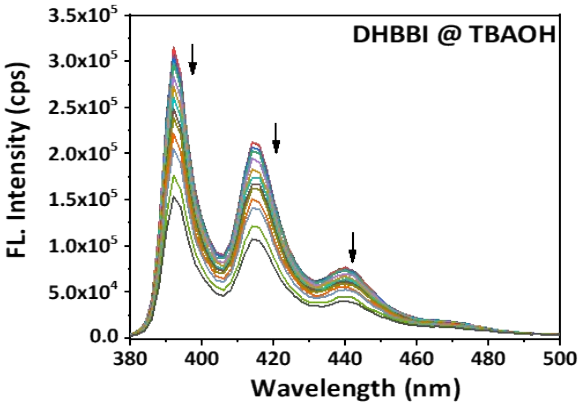
DHBBI @ TBAOH
FL. Intensity (cps)
Wavelength (nm)

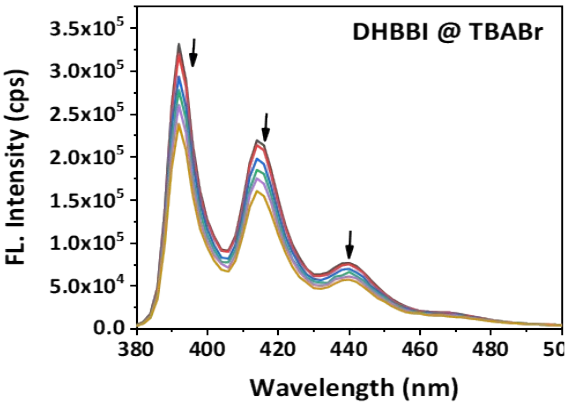
DHBBI @ TBABr
FL. Intensity (cps)
Wavelength (nm)

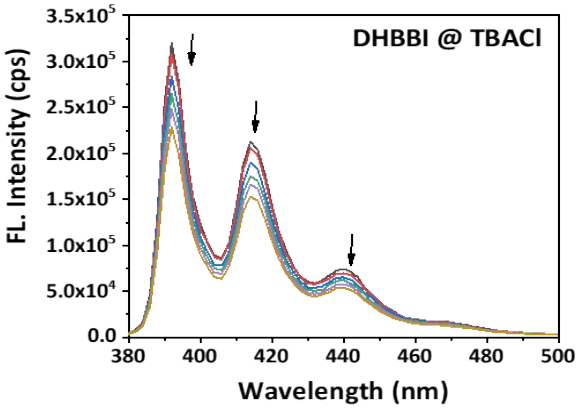
DHBBI @ TBACl
FL. Intensity (cps)
Wavelength (nm)

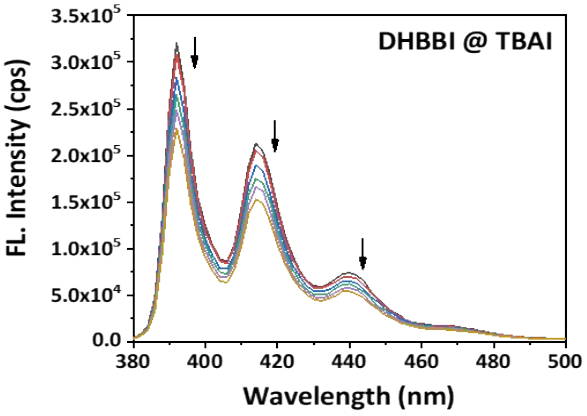
DHBBI @ TBAI
FL. Intensity (cps)
Wavelength (nm)

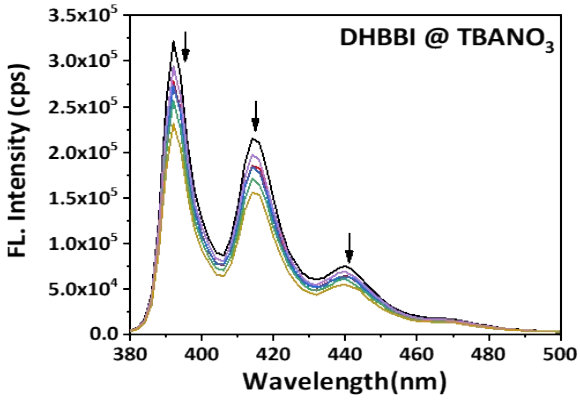
DHBBI @ TBANO3
FL. Intensity (cps)
Wavelength(nm)

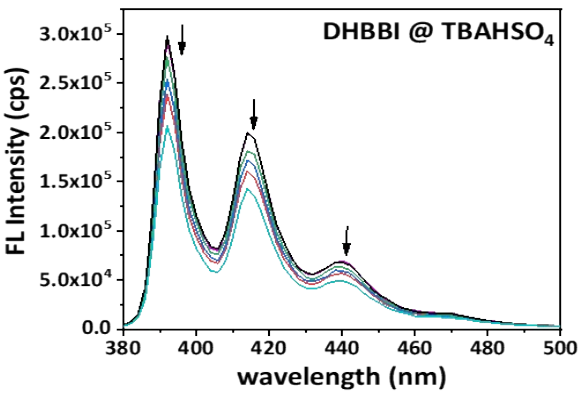
DHBBI @ TBAHSO4
FL Intensity (cps)
wavelength (nm)

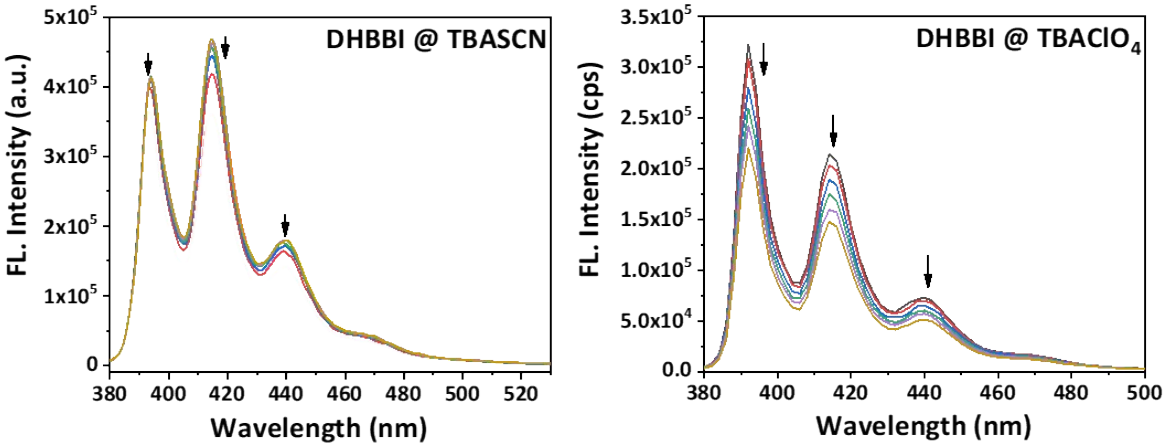

Fig. S15. Fluorescence quenching behaviour of DHBBI with different anionic analytes in ACN.

Table S5. Summary of the calculated K_{sv} values (M^{-1}) of different DHBBI and its derivatives with various anion analytes.

Analyte	DHBBI	DHBBI-OH	2-DHBBI-OH	DHBBI-Hex
TBAF	$11.6x10^4$	$8.82x10^4$	$6.67 x10^4$	2.93×10^4
TBACN	$10.2x10^4$	$8.02x10^4$	$7.25x10^4$	7.95×10^4
TBAOH	$9.38x10^4$	$8.30x10^4$	$8.30x10^4$	6.58×10^4
TBABr	$7.94x10^4$	$6.85x10^4$	$8.68x10^4$	8.86×10^4
TBACl	$8.27x10^4$	$6.62x10^4$	$5.27x10^4$	6.99×10^4
TBAI	$7.99x10^4$	$8.25x10^4$	$2.68x10^4$	6.63×10^4
$TBANO_3$	$8.27x 10^4$	$7.62x10^4$	$5.52x10^4$	6.57×10^4
$TBAHSO_4$	$5.37x 10^4$	$7.71x10^4$	$8.23x10^4$	6.27×10^4
$TBAClO_4$	$8.97x 10^4$	$7.71x10^4$	$6.92x10^4$	4.68×10^4
TBASCN	$4.86x10^4$	$5.94 x10^4$	$4.68x10^4$	$6.55x10^4$

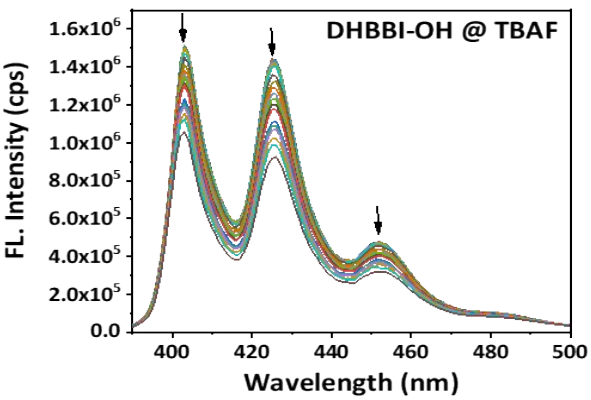
DHBBI-OH @ TBAF
FL. Intensity (cps)
Wavelength (nm)

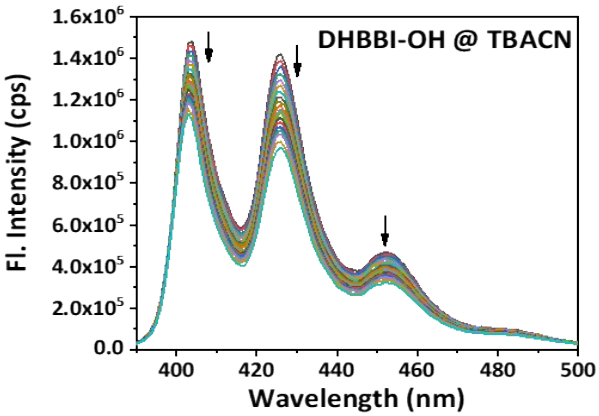
DHBBI-OH @ TBACN
Fl. Intensity (cps)
Wavelength (nm)

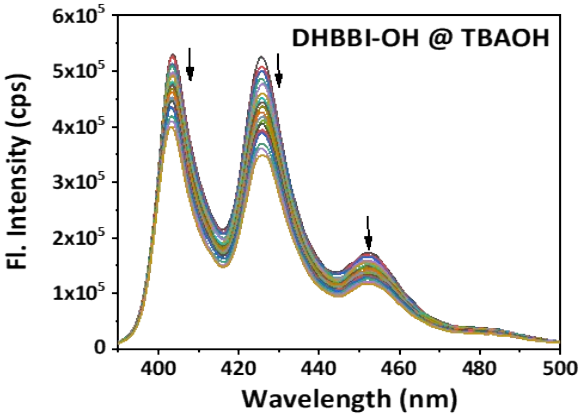
DHBBI-OH @ TBAOH
Fl. Intensity (cps)
Wavelength (nm)

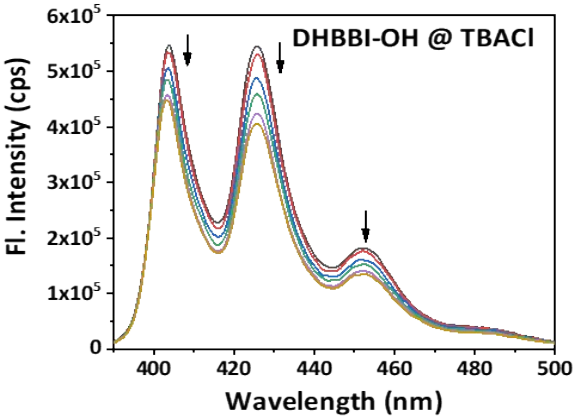
DHBBI-OH @ TBACl
Fl. Intensity (cps)
Wavelength (nm)

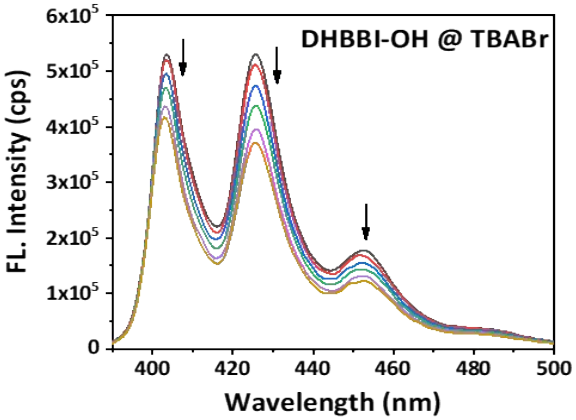
DHBBI-OH @ TBABr
FL. Intensity (cps)
Wavelength (nm)

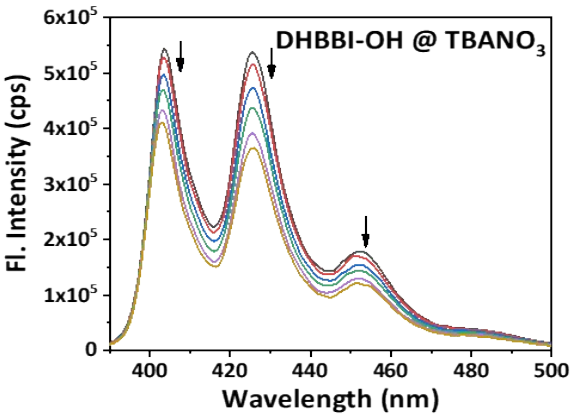
DHBBI-OH @ TBANO3
Fl. Intensity (cps)
Wavelength (nm)

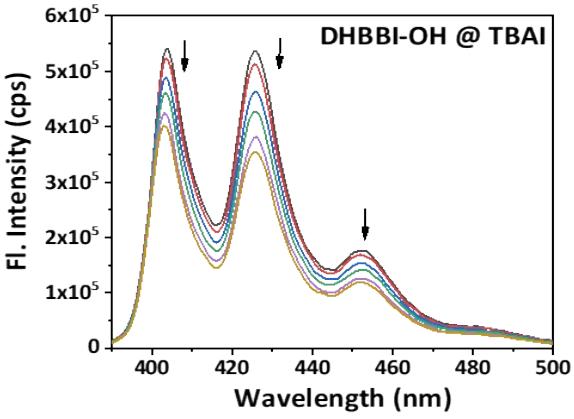
DHBBI-OH @ TBAI
Fl. Intensity (cps)
Wavelength (nm)

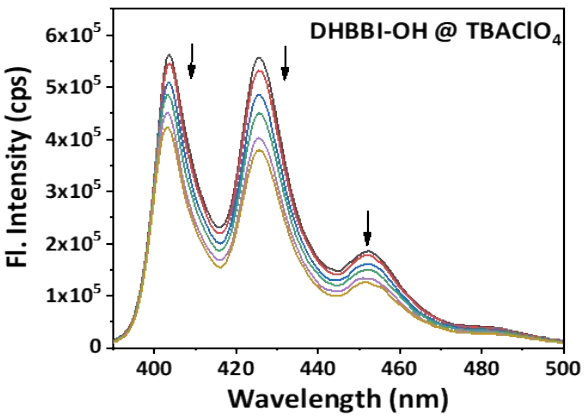
DHBBI-OH @ TBAClO4
Fl. Intensity (cps)
Wavelength (nm)

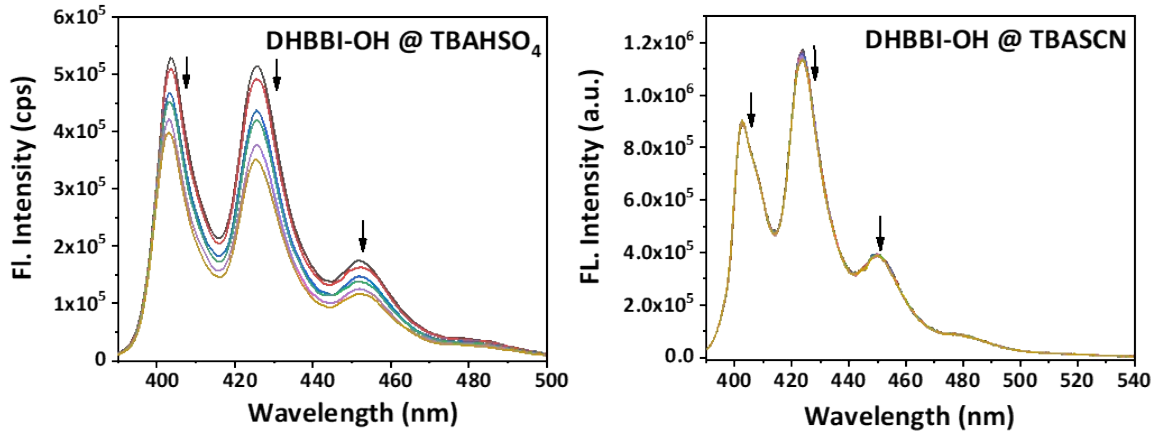

Fig. S16. Fluorescence quenching behaviour of DHBBI-OH with different anionic analytes in ACN.

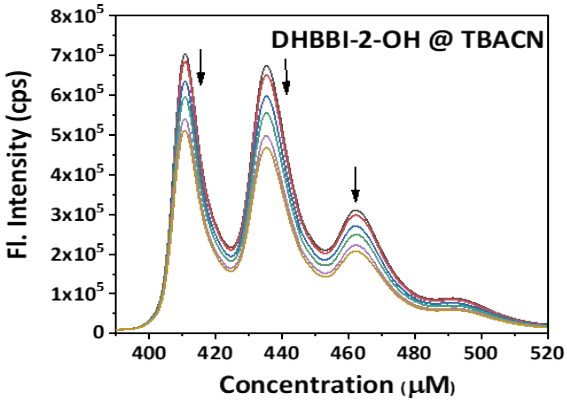
DHBBI-2-OH @ TBACN
Fl. Intensity (cps)
Concentration (μM)

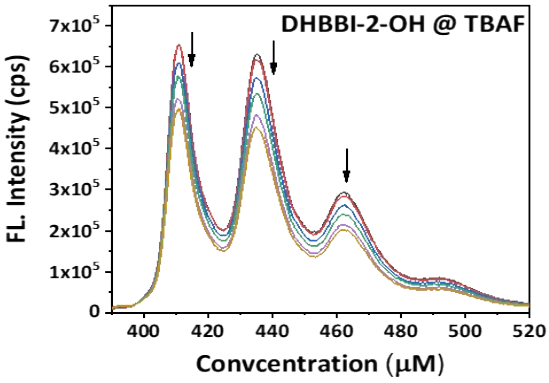
DHBBI-2-OH @ TBAF
FL. Intensity (cps)
Convcentration (μM)

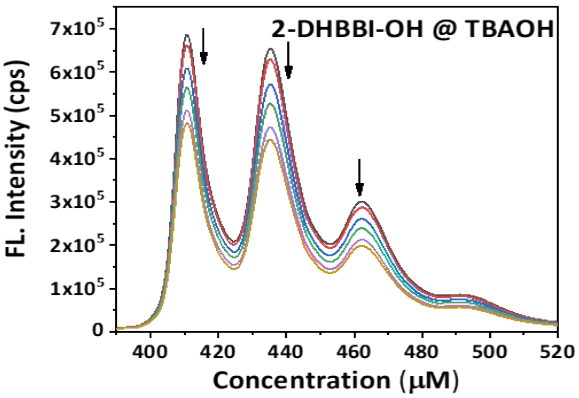
2-DHBBI-OH @ TBAOH
FL. Intensity (cps)
Concentration (μM)

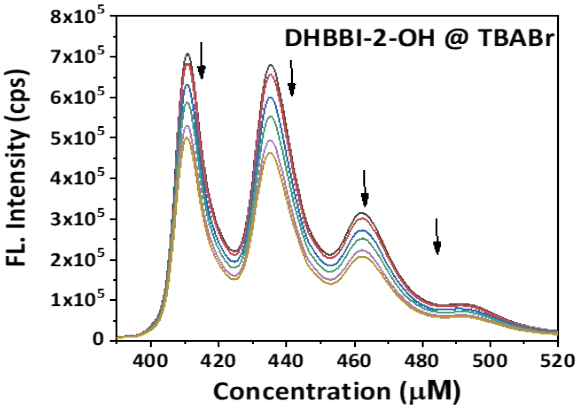
DHBBI-2-OH @ TBABr
FL. Intensity (cps)
Concentration (μM)

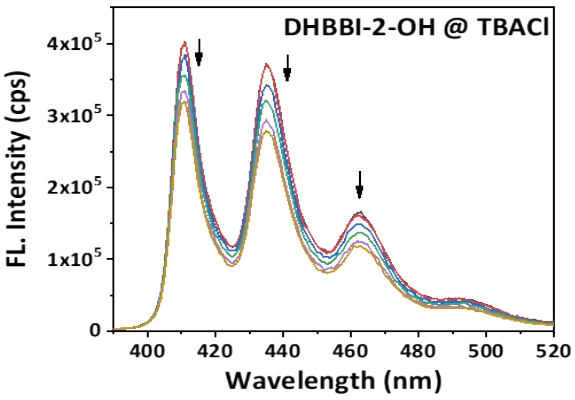
DHBBI-2-OH @ TBACl
FL. Intensity (cps)
Wavelength (nm)

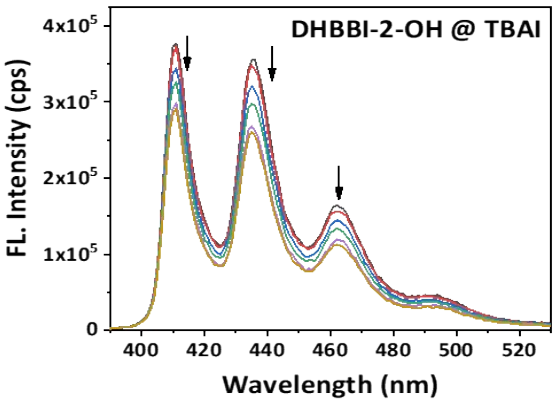
DHBBI-2-OH @ TBAI
FL. Intensity (cps)
Wavelength (nm)

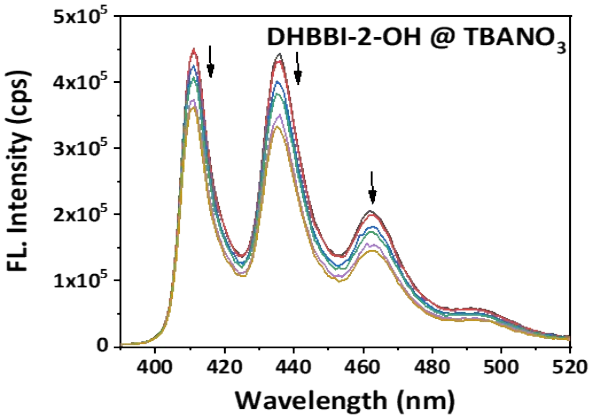
DHBBI-2-OH @ TBANO3
FL. Intensity (cps)
Wavelength (nm)

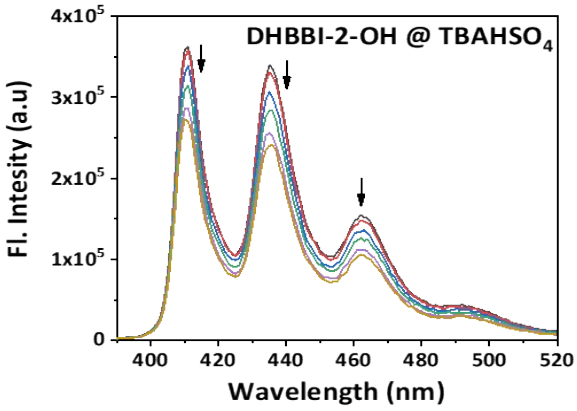
DHBBI-2-OH @ TBAHSO4
Fl. Intesity (a.u)
Wavelength (nm)

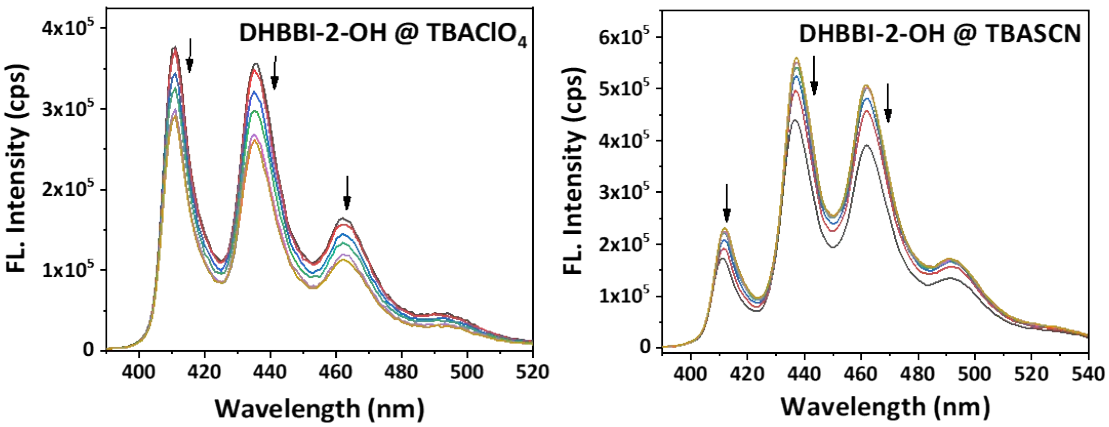

Fig. S17. Fluorescence quenching behaviour of DHBBI-2-OH with different anionic analytes in ACN.

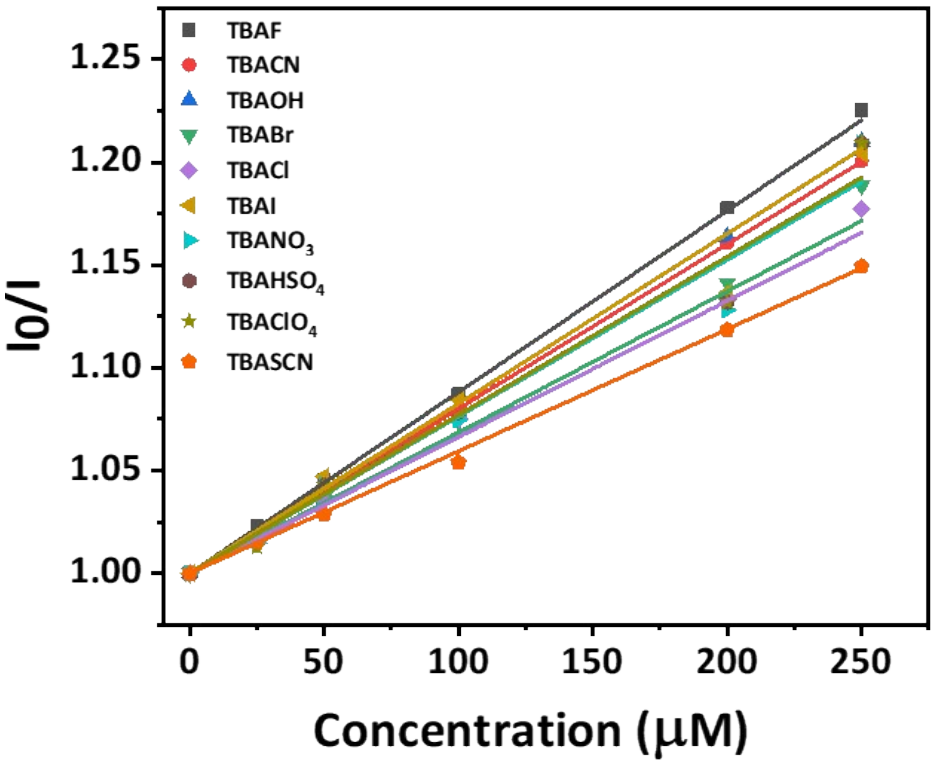

Fig. S18. Comparison in the Stern-Volmer plot of DHBBI-OH with different anion analytes.

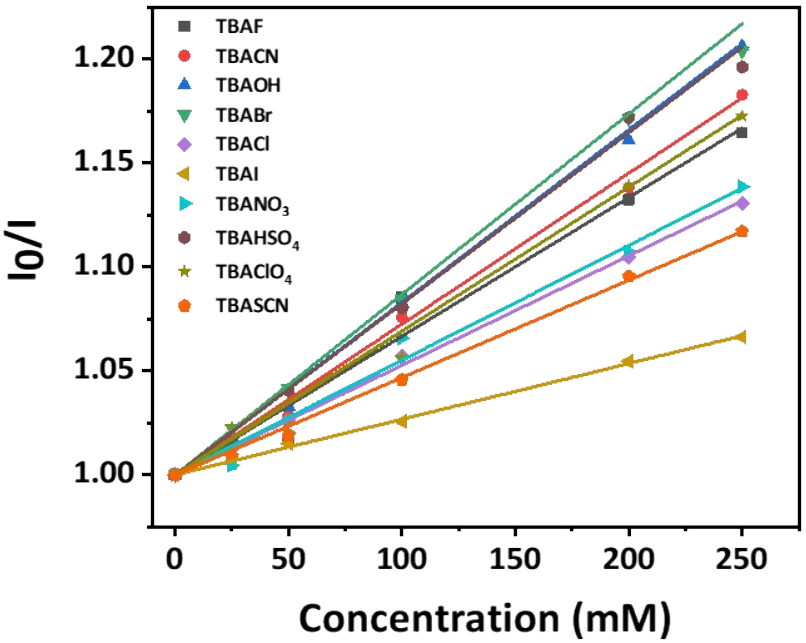

Fig. S19. Comparison in the Stern-Volmer plot of DHBBI-2-OH with different anion analytes.

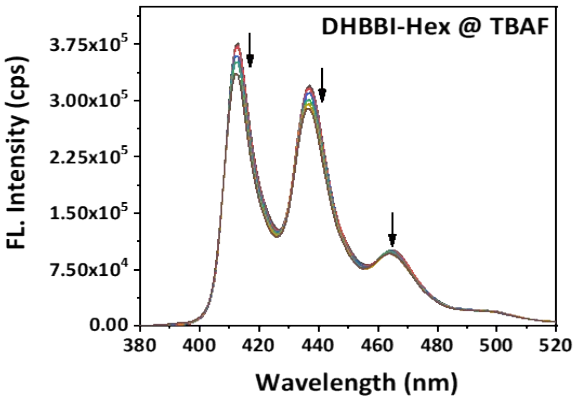
DHBBI-Hex @ TBAF
FL. Intensity (cps)
Wavelength (nm)

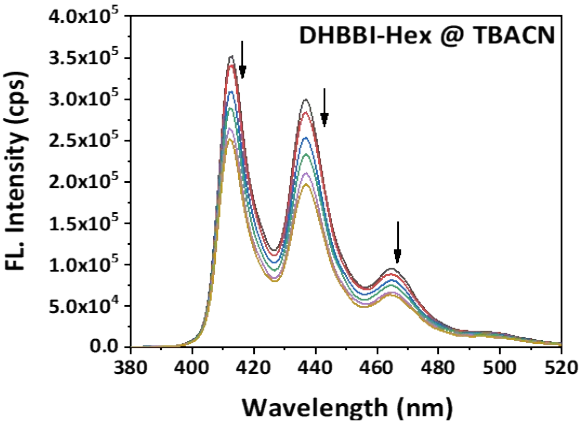
DHBBI-Hex @ TBACN
FL. Intensity (cps)
Wavelength (nm)

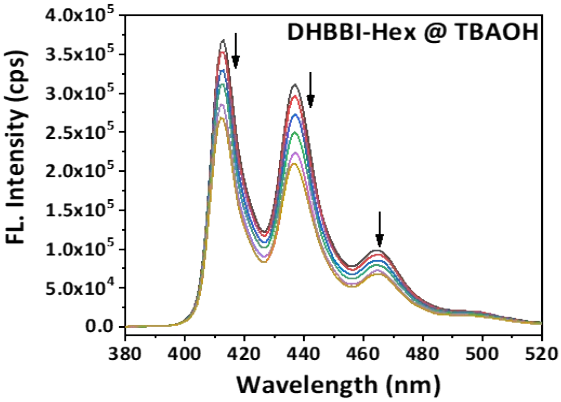
DHBBI-Hex @ TBAOH
FL. Intensity (cps)
Wavelength (nm)

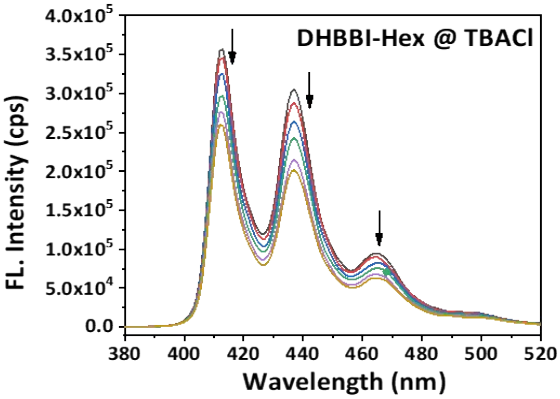
DHBBI-Hex @ TBACl
FL. Intensity (cps)
Wavelength (nm)

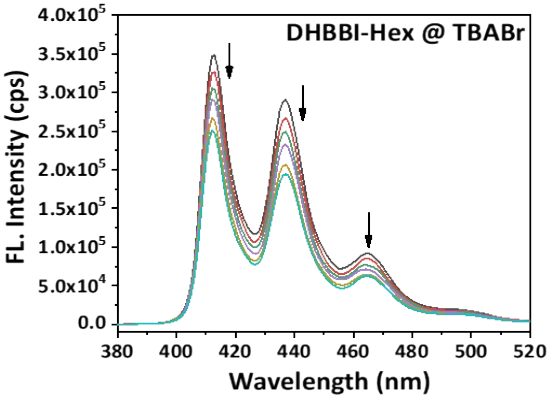
DHBBI-Hex @ TBABr
FL. Intensity (cps)
Wavelength (nm)

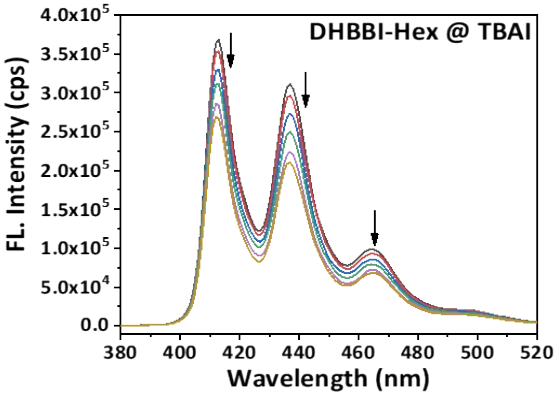
DHBBI-Hex @ TBAI
FL. Intensity (cps)
Wavelength (nm)

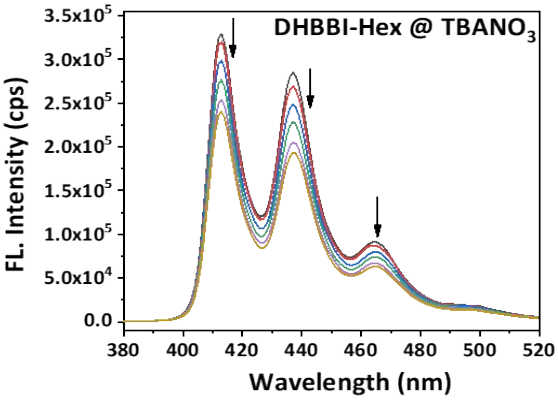
DHBBI-Hex @ TBANO3
FL. Intensity (cps)
Wavelength (nm)

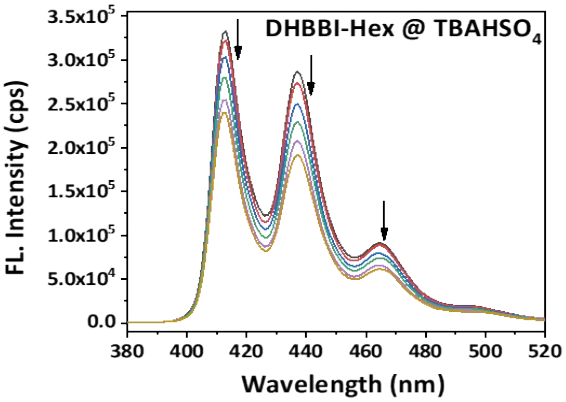
DHBBI-Hex @ TBAHSO4
FL. Intensity (cps)
Wavelength (nm)

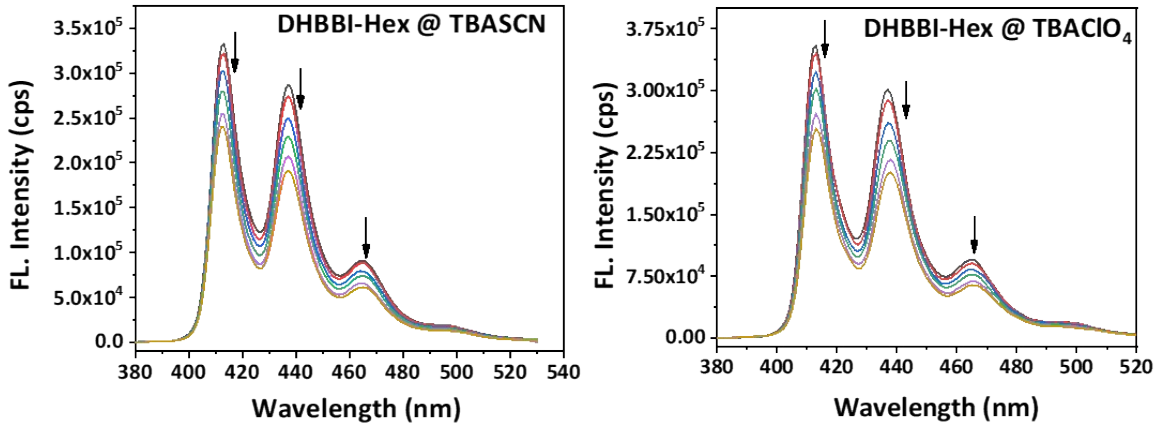

Fig. S20. Fluorescence quenching behaviour of DHBBI-Hex with different anionic analytes in ACN.

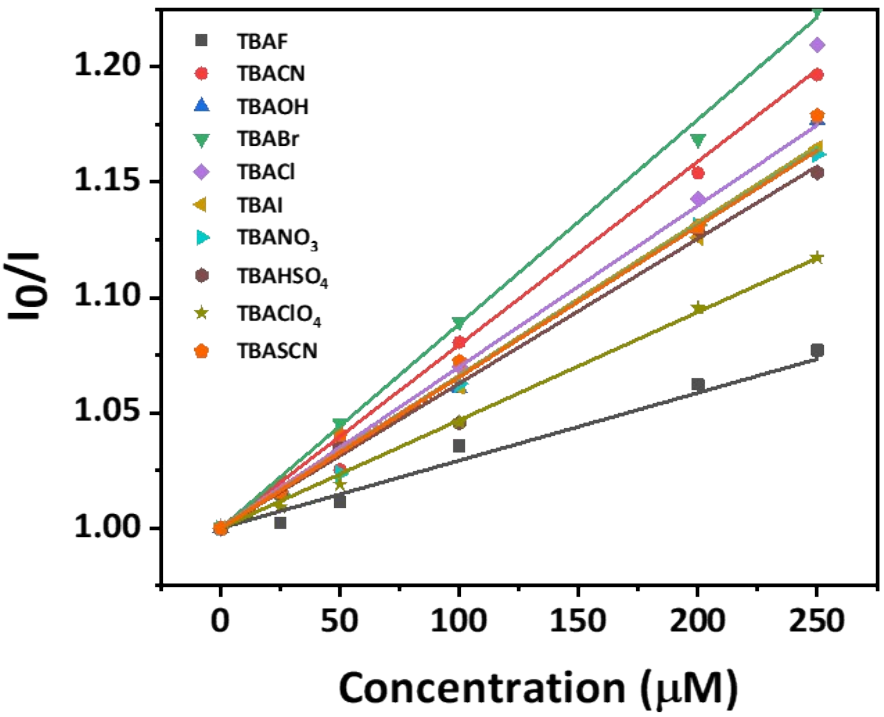

Fig. S21. Comparison in the Stern-Volmer plot of DHBBI-Hex with different anion analytes.

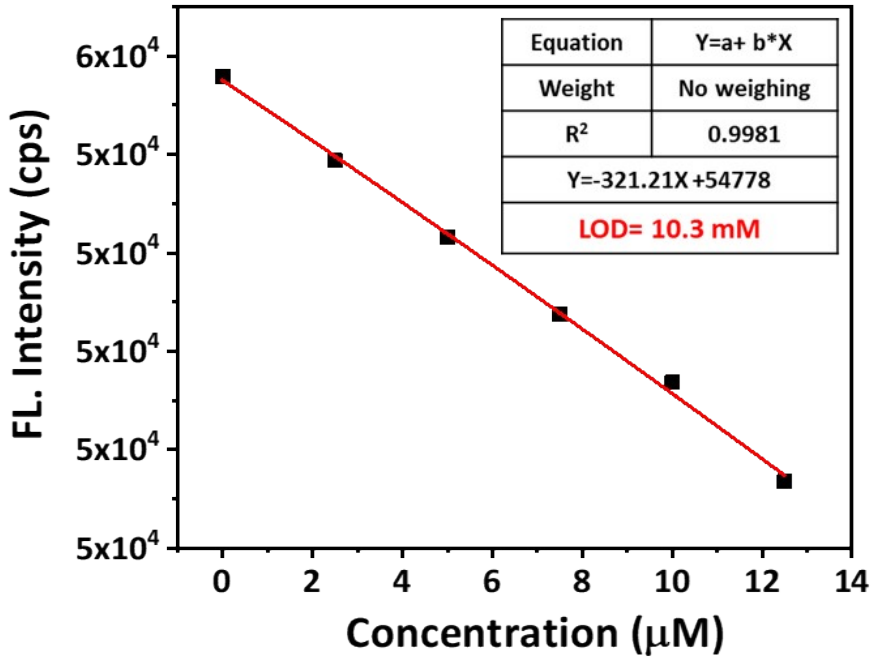

Fig. S22. Change in the emission intensity of DHBBI at different F^- concentrations.

Table S6. Summary of the calculated lifetime values of different DHBBI with F^- anion.

Compound Name	T (ns)	χ^2
DHBBI	1.905	1.0130
DHBBI: TBAF (1:0.1)	1.895	1.0844
DHBBI: TBAF (1:0.25)	2.000	1.1242
DHBBI: TBAF (1:0.50)	1.972	1.0663
DHBBI: TBAF (1:0.75)	2.015	1.1341
DHBBI: TBAF (1:1)	2.054	1.0049
DHBBI: TBAF (1:2)	2.084	1.1719
DHBBI: TBAF (1:5)	2.358	1.0043

Table S7. Comparison of DHBBI with already reported F^- responsive probes

S. No	Compound Name	Medium	Binding constant	Ref.
1	4-(Dimethylamino)salicylaldehyde	ACN	$4.13 \times 10^4\ M^{-1}$	1
2	2-(2-(dimethylamino)ethylamino)-3-chloronaphthalene-1,4-dione (R1) and its Zn metal chelates $[Zn(R1)Cl_2]$	DMF	$6.2 \times 10^4\ M^{-1}$	2
3	2,3-di(1H-2-pyrrolyl)-7,12-dihydronaphtho[2,3-f]quinoxaline-7,12-dione	DMSO/DCM	$1.6 \times 10^4\ M^{-1}$	3
4	10-(6-Amino-1,3-dimethyl-2,4-dioxo-1,2,3,4-tetrahydro-pyrimidin-5-yl)-1,3-dimethyl-1,10-dihydro-9-oxa-1,3-diaza-anthracene-2,4-dione (1)	ACN	$3.15 \times 10^4\ M^{-1}$	4
5	2-(4-Nitro-phenyl)-4,5-diphenyl-1H-imidazole	ACN:H_2O	$1.42 \times 10^4\ M^{-1}$	5
6	2,7-dihydrobenzo[1,2,3-cd:4,5,6-c'd']bis(indazole) (DHBBI)	ACN	$11.6 \times 10^4\ M^{-1}$	This present work

References

1 K. Liu, X. Zhao, Q. Liu, J. Huo, H. Fu and Y. Wang, Turn on ESPT: Novel salicylaldehyde based sensor for biological important fluoride sensing, *J. Photochem. Photobiol. B Biol.*,

2014, **138**, 75–79.

2 C. Parthiban and K. P. Elango, Amino-naphthoquinone and its metal chelates for selective sensing of fluoride ions, *Sens. Actuators B Chem.*, 2015, **215**, 544–552.

3 T. Ghosh, B. G. Maiya and M. W. Wong, Fluoride Ion receptors based on dipyrrolyl derivatives bearing electron-withdrawing groups: Synthesis, optical and electrochemical sensing, and computational studies, *J. Phys. Chem. A*, 2004, **108**, 11249–11259.

4 N. Kaur and G. Jindal, "Switch on" fluorescent sensor for the detection of fluoride ions in solution and commercial tooth paste, *Spectrochim. Acta Part A Mol. Biomol. Spectrosc.*, 2019, **223**, 117361.

5 S. Goswami and R. Chakrabarty, An imidazole-based colorimetric sensor for fluoride anion, *Eur. J. Chem.*, 2011, **2**, 410–415.